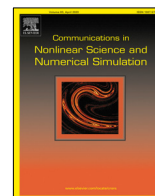




Contents lists available at ScienceDirect

# Communications in Nonlinear Science and Numerical Simulation

journal homepage: [www.elsevier.com/locate/cnsns](http://www.elsevier.com/locate/cnsns)

Research paper

## Diffusibility of a kind of quasi-star higher-order network

Bo Li<sup>a</sup>, Jin Zhou<sup>a,b,\*</sup>, Weiqiang Li<sup>c</sup>, Jun-an Lu<sup>a</sup><sup>a</sup> School of Mathematics and Statistics, Wuhan University, Hubei 430072, China<sup>b</sup> Hubei Key Laboratory of Computational Science, Wuhan University, Hubei 430072, China<sup>c</sup> School of Mathematics, North University of China, Shanxi 030051, China

### ARTICLE INFO

#### Article history:

Received 8 February 2023

Received in revised form 4 August 2023

Accepted 11 August 2023

Available online 22 August 2023

#### Keywords:

Complex network

Higher-order network

Diffusibility

Optimization

### ABSTRACT

Real life networks heavily rely on higher-order interactions. This paper studies the diffusibility of novel quasi-star higher-order networks from two aspects. When the coupling strengths of the lower-order and higher-order coupling parts are less than 1, the diffusibility can be maximized by choosing the intermediate values of these coupling strengths. When they are far greater than 1, there exists an inferior limit of the diffusibility, and the lower-order coupling part has more impact on quasi-star network's diffusibility. Additionally, the face with the middle order in the higher-order coupling part plays a more important role in enhancing the network's diffusibility compared with other faces, and the diffusibility does not naturally increase with the order of face. These results give us some insights into the influence of higher-order structures and their faces.

© 2023 Elsevier B.V. All rights reserved.

## 1. Introduction

In recent decades, simple networks with pairwise interactions have been extensively applied to various fields of research: control [1–3], synchronization [4,5], game [6], diffusion [7], topology identification [8], and spread [9]. However, real life interactions are higher-order ones instead of pairwise ones which involve more than two individuals. For example, in a Borromean ring [10], three rings cannot be separated without cutting; but once any one of them is removed, the other two can be pulled apart without any further cutting. Numerous nerve cells cooperate through higher-order interactions to carry out a task in the neural networks of the human brain and *C. elegans*. Simplicial complexes and hypergraphs are two common higher-order network models used to represent these complex phenomena [11–15].

Very recently, the dynamical processes that arise on higher-order networks were thoroughly explored [16,17]. Gambuzza proposed an adapted master stability function method for analyzing the synchronizability of a simplicial complex [18], and Gallo further extended this method to a directed higher-order hypergraph [19]. Moreover, Lucas introduced higher-order Laplacian matrices [20], and Torres investigated the spectral properties of Laplacian matrices corresponding to a simplicial complex model.

There is an amount of information hidden behind the Laplacian matrices. For example, the second smallest Laplacian eigenvalue, named the spectral gap, plays an important role in the analysis of the dynamics of complex networks [18,19, 21–23], denoted as  $\lambda_2$ . The diffusion of substances distributed to nodes of the simple network flow from nodes with higher concentrations to nodes with lower concentrations [16]. The correlation time scale is usually called the relaxation time  $\tau$ , which is an index of the network diffusion. For a connected network, the relaxation time of the network is commonly given as the reciprocal of the spectral gap [24,25], i.e.  $\tau \propto 1/\lambda_2$ . Naturally, the larger the value of the spectral gap, the faster

\* Corresponding author at: School of Mathematics and Statistics, Wuhan University, Hubei 430072, China.

E-mail addresses: [lib2020@whu.edu.cn](mailto:lib2020@whu.edu.cn) (B. Li), [jzhou@whu.edu.cn](mailto:jzhou@whu.edu.cn) (J. Zhou), [20220095@nuc.edu.cn](mailto:20220095@nuc.edu.cn) (W. Li), [jalu@whu.edu.cn](mailto:jalu@whu.edu.cn) (J. Lu).

the diffusion rate. For higher-order networks, these substances can be distributed not only on nodes (0-order simplexes) but also on edges (1-order simplexes), triangles (2-order simplexes) and tetrahedrons (3-order simplexes), etc. Similar to this, higher-order Laplacian matrices are used to study the diffusibility of higher-order networks.

Topology and function are essential in biology. Higher-order interactions, namely simplexes or hyperedges, are generally found in many biological networks, such as brain network [26]. Functions of brain are significantly affected by remote synchronization, which is popular in quasi-star coupling structure [27,28]. To depict this type of topology, a higher-order quasi-star network with a hub and multiple simplexes is investigated. In this paper, we draw some interesting conclusions on the diffusibility of this type of higher-order networks. We find that the diffusibility of the quasi-star networks can be maximized by choosing appropriate coupling strengths if both the coupling strengths of the lower-order and higher-order coupling parts are less than 1. On the other hand, when the coupling strengths are far greater than 1, there exist lower bounds of the diffusibility of the quasi-star networks. Further, considering that the higher-order coupling part is comprised of some faces, the impact of faces on the diffusibility is discussed in the two cases above.

The structure of this paper is as follows. In Section 2, we propose the model of quasi-star higher-order networks. The diffusibility of the quasi-star networks is investigated in Sections 3 and 4. Further discussion and a summary of conclusions are stated in Sections 5 and 6 respectively.

## 2. Preliminaries and model

### 2.1. Mathematical preliminaries

To get our main results, some basic concepts [11] are stated below.

**Definition 1 (Simplex).** A  $d$ -order simplex is composed of the interaction of a set of  $d + 1$  nodes  $v_1, \dots, v_{d+1}$ , denoted as  $[v_1, \dots, v_{d+1}]$ , so a 0-order simplex represents the interaction between a node and itself, a 1-order simplex represents the pairwise interaction between two nodes, and a 2-order simplex represents the many-body interaction among three nodes, etc.

**Definition 2 (Face).** The face of a  $d$ -order simplex  $[v_1, \dots, v_{d+1}]$  is formed by the interaction of the subsets of its nodes. For example, the faces of a 2-order simplex are three 0-order simplexes (nodes), three 1-order simplexes (edges), and a 2-order simplex (triangle).

**Definition 3 (Simplicial Complex).** A simplicial complex is made up of a set of simplexes that are closed concerning their faces. The highest order of the simplex in the simplicial complex is defined as the order of the higher-order network.

**Definition 4 (Facet).** A facet is a simplex of a simplicial complex, but it is not a face of any other simplex. Therefore, all facets of a simplicial complex completely decide its structure.

### 2.2. Model

Quasi-star higher-order networks are considered in this paper, which consist of a central node and a number of simplexes. A 3-order quasi-star network with 5 3-order simplexes (where  $T = 5$  and  $m - 1 = 3$ ) is shown in Fig. 1 as an example. Higher-order networks considered here are locally homogeneous but globally heterogeneous. The diffusion dynamics on a quasi-star higher-order network with  $T$  ( $m - 1$ )-order simplexes are described by

$$\begin{aligned} \dot{\mathbf{x}}_i &= a_0 \sum_{j_0=1}^{mT+1} A_{ij_0}^{(0)} \mathbf{h}^{(0)}(\mathbf{x}_i, \mathbf{x}_{j_0}) + a_1 \sum_{j_1=1}^{mT+1} A_{ij_1}^{(1)} \mathbf{h}^{(1)}(\mathbf{x}_i, \mathbf{x}_{j_1}) \\ &+ a_2 \sum_{j_1, j_2=1}^{mT+1} A_{ij_1 j_2}^{(2)} \mathbf{h}^{(2)}(\mathbf{x}_i, \mathbf{x}_{j_1}, \mathbf{x}_{j_2}) + \dots \\ &+ a_{m-1} \sum_{j_1, \dots, j_{m-1}=1}^{mT+1} A_{ij_1 \dots j_{m-1}}^{(m-1)} \mathbf{h}^{(m-1)}(\mathbf{x}_i, \mathbf{x}_{j_1}, \dots, \mathbf{x}_{j_{m-1}}), \\ &i = 1, 2, \dots, mT + 1, \end{aligned} \tag{1}$$

where  $\mathbf{x}_i$  indicates the states of the node  $i$ ,  $a_0 > 0$  is the coupling strength of the pairwise interaction of two nodes in the lower-order coupling part, and  $a_d > 0$  ( $d = 1, \dots, m - 1$ ) is the coupling strength of the pairwise or many-body interaction of  $d + 1$  nodes in the higher-order coupling part,  $\mathbf{h}^{(d)} : \mathbb{R}^{(d+1) \times n} \rightarrow \mathbb{R}^n$  describes the coupling function of  $d + 1$  nodes, satisfying  $\mathbf{h}^{(d)}(\mathbf{x}, \mathbf{x}, \dots, \mathbf{x}) \equiv 0$  for any  $\mathbf{x} \in \mathbb{R}^n$ . Both  $A_{ij_0}^{(0)}$  and  $A_{ij_1 \dots j_d}^{(d)}$  ( $d = 1, \dots, m - 1$ ) are adjacency tensors representing the topology of the network [18,20,23,29–31]. In general, if two nodes, say  $i$  and  $j_1$  (or  $j_0$ ), interact, then

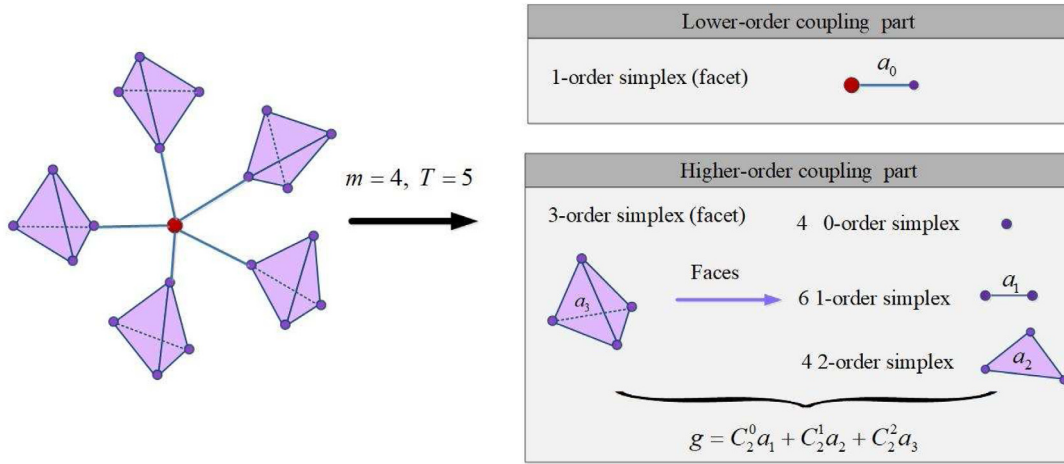


**Fig. 1.** Schematic diagram of a 3-order quasi-star network consisting of five lower-order coupling parts, five higher-order coupling parts, and its faces.

$A_{ij_1}^{(1)} = 1$  (or  $A_{ij_0}^{(0)} = 1$ ); otherwise,  $A_{ij_1}^{(1)} = 0$  (or  $A_{ij_0}^{(0)} = 0$ ). Furthermore, if there are many-body interactions among nodes  $i, j_1, \dots, j_d$ , then  $A_{ij_1 \dots j_d}^{(d)} = 1$ ; otherwise,  $A_{ij_1 \dots j_d}^{(d)} = 0$ .

As a powerful tool for studying complex networks, Laplacian matrices can be generalized to higher-order networks. The  $(i, j)$  element of the  $d$ -order Laplacian matrix of a  $(m - 1)$ -order simplicial complex can be described by  $L_{ij}^{(d)} = dP_i^{(d)}\delta_{ij} - Q_{ij}^{(d)}$  ( $1 \leq i, j \leq N$ ), where  $N$  denotes the size of the network,  $P_i^{(d)} = \frac{1}{d!} \sum_{j_1, \dots, j_d=1}^N A_{ij_1 \dots j_d}^{(d)}$  denotes the number of distinct  $d$ -order simplexes in which node  $i$  participates, and  $Q_{ij}^{(d)} = \frac{1}{(d-1)!} \sum_{j_1, \dots, j_{d-1}=1}^N A_{ijj_1 \dots j_{d-1}}^{(d)}$  represents the number of distinct  $d$ -order simplexes in which node  $i$  and node  $j$  participate. If  $i = j$ , then  $\delta_{ij} = 1$ ; otherwise,  $\delta_{ij} = 0$ . The multi-order Laplacian matrix corresponding to the  $(m - 1)$ -order simplicial complex [18] is defined as

$$\mathcal{L} = \sum_{j=0}^{m-1} a_j L^{(j)}, \tag{2}$$

where  $a_0 L^{(0)} + a_1 L^{(1)}$  and  $a_j L^{(j)}$  represent the weighted 1-order and  $j$ -order Laplacian matrices, respectively.

For a quasi-star network with  $T$   $(m - 1)$ -order simplexes, the  $d$ -order Laplacian matrix has the following form

$$L_{(mT+1) \times (mT+1)}^{(d)} = \left( \begin{array}{c|c} O_{1 \times 1}^{(d)} & S_{1 \times mT}^{(d)} \\ \hline (S_{1 \times mT}^{(d)})^\top & D_{mT \times mT}^{(d)} \end{array} \right), \tag{3}$$

where  $D_{mT \times mT}^{(d)} = \text{diag}\{\mathfrak{D}_{m \times m}^{(d)}, \mathfrak{D}_{m \times m}^{(d)}, \dots, \mathfrak{D}_{m \times m}^{(d)}\}$ , and

$$\mathfrak{D}_{m \times m}^{(d)} = \begin{pmatrix} (m-1)C_{m-2}^{d-1} & -C_{m-2}^{d-1} & -C_{m-2}^{d-1} & \dots & -C_{m-2}^{d-1} \\ -C_{m-2}^{d-1} & (m-1)C_{m-2}^{d-1} & -C_{m-2}^{d-1} & \dots & -C_{m-2}^{d-1} \\ \vdots & \vdots & \vdots & \ddots & \vdots \\ -C_{m-2}^{d-1} & -C_{m-2}^{d-1} & -C_{m-2}^{d-1} & \dots & (m-1)C_{m-2}^{d-1} \end{pmatrix}.$$

Similarly, if  $d = 1$ , the block matrices of  $a_0 L^{(0)} + a_1 L^{(1)}$  are  $O_{1 \times 1}^{(1)} = Ta_0$ ,  $S_{1 \times mT}^{(1)} = (-a_0 \ 0 \ 0 \ \dots \ 0; -a_0 \ 0 \ 0 \ \dots \ 0; \dots; -a_0 \ 0 \ 0 \ \dots \ 0)$ ,  $D_{mT \times mT}^{(1)} = \text{diag}\{\mathcal{D}_{m \times m}^{(1)}, \mathcal{D}_{m \times m}^{(1)}, \dots, \mathcal{D}_{m \times m}^{(1)}\}$ , and  $\mathcal{D}_{m \times m}^{(1)} = a_1 \mathfrak{D}_{m \times m}^{(1)} + \text{diag}\{a_0 \ 0 \ 0 \ \dots \ 0; a_0 \ 0 \ 0 \ \dots \ 0; \dots; a_0 \ 0 \ 0 \ \dots \ 0\}$ , respectively; else if  $d = 2, \dots, m - 1$ , the block matrices of  $a_d L^{(d)}$  are  $O_{1 \times 1}^{(d)} = 0$ ,  $S_{1 \times mT}^{(d)} = (0 \ 0 \ 0 \ \dots \ 0; 0 \ 0 \ 0 \ \dots \ 0; \dots; 0 \ 0 \ 0 \ \dots \ 0)$ ,  $D_{mT \times mT}^{(d)} = \text{diag}\{\mathcal{D}_{m \times m}^{(d)}, \mathcal{D}_{m \times m}^{(d)}, \dots, \mathcal{D}_{m \times m}^{(d)}\}$ , and  $\mathcal{D}_{m \times m}^{(d)} = a_d \mathfrak{D}_{m \times m}^{(d)}$ .

By Lemma 1 [32] (see Appendix A), the characteristic polynomial of  $\mathcal{L}$  is simplified as  $|\lambda I - \mathcal{L}| = \lambda[\lambda - (a_0 + mg \pm \sqrt{\Delta_1})/2]^{2(T-1)}[\lambda - (a_0 + mg + Ta_0 \pm \sqrt{\Delta_2})/2]^2(\lambda - mg)^{(m-2)T}$ . Here,  $\Delta_1 = (a_0 + mg)^2 - 4a_0g$ ,  $\Delta_2 = (a_0 + Ta_0 + mg)^2 - 4(1 + mT)a_0g$ , and  $g = \sum_{k=1}^{m-1} a_k C_{m-2}^{k-1}$  represents the compound coupling strength of the higher-order coupling part composed of the  $(m - 1)$ -order facet and its faces, as shown in Fig. 1. As a result, the second smallest eigenvalue of the Laplacian matrix  $\mathcal{L}$  is

$$\lambda_2^h = \frac{a_0 + mg - \sqrt{\Delta_1}}{2}. \tag{4}$$

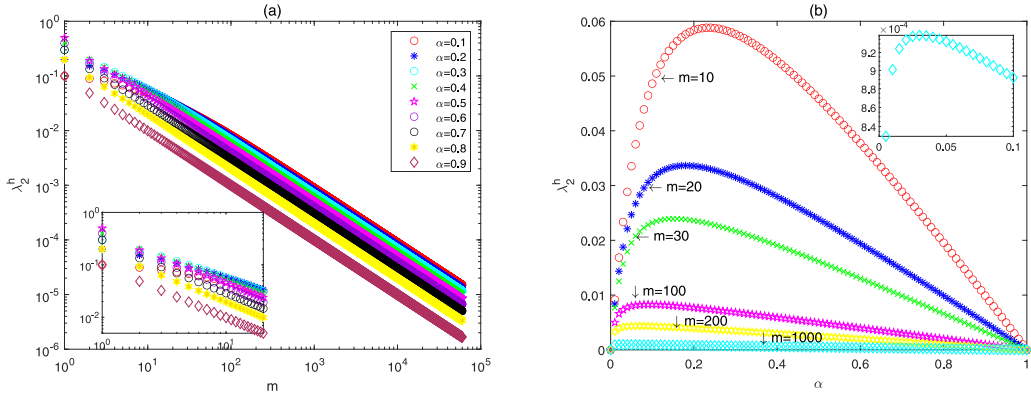


**Fig. 2.** The diffusibility of an  $(m - 1)$ -order quasi-star network. (a) The curves of  $\lambda_2^h$  versus  $m$  for various values of  $\alpha$ . (b) The inverted U-shaped curves of  $\lambda_2^h$  versus  $\alpha$  for various values of  $m$ .

Clearly, the value of  $\lambda_2^h$  depends on  $a_0$ ,  $m$ , and  $g$ . To explore the diffusibility of quasi-star higher-order networks, the sensitivity of  $\lambda_2^h$  to  $a_0$  and  $g$  is investigated, where  $a_0$  and  $g$  correspond to the lower-order and higher-order coupling parts respectively. Below, we discuss two cases:  $a_0, g \in (0, 1)$  and  $a_0 \gg 1, g \gg 1$  in detail.

**3. Case I:  $a_0, g \in (0, 1)$**

To illustrate which one has more impact on the diffusibility of an  $(m - 1)$ -order quasi-star network, the lower-order coupling part  $a_0$  or the higher-order coupling part  $g$ , we first consider the case of  $a_0 + g = 1$ . For simplicity, assume that  $g = \alpha$  and  $\alpha \in (0, 1)$ .

**3.1. The lower-order and higher-order coupling parts**

From Eq. (4), the spectral gap is

$$\lambda_2^h(\alpha, m) = \frac{1 - \alpha + m\alpha - \sqrt{(1 - \alpha + m\alpha)^2 - 4\alpha(1 - \alpha)}}{2}. \tag{5}$$

It can be easily demonstrated that  $\lambda_2^h(\alpha, m_1) < \lambda_2^h(\alpha, m_2)$  if  $m_1 > m_2$ , and  $\lim_{m \rightarrow +\infty} \lambda_2^h(\alpha, m) = 0$ , which implies that the spectral gap converges decreasingly to 0 as  $m$  increases. Fig. 2(a) tells the relation between  $\lambda_2^h$  and  $m$  for various values of  $\alpha$ .

On the other hand, according to Eq. (5), the first and second derivatives of  $\lambda_2^h(\alpha, m)$  with respect to  $\alpha$  are

$$\frac{\partial \lambda_2^h(\alpha, m)}{\partial \alpha} = \frac{1}{2} \left( m - 1 - \frac{p_1}{q_1} \right), \tag{6}$$

and

$$\frac{\partial^2 \lambda_2^h(\alpha, m)}{\partial \alpha^2} = \frac{p_1^2 - [(m - 1)^2 + 4]q_1^2}{2q_1^3} = \frac{2 - 2m}{q_1^3}, \tag{7}$$

respectively, where  $p_1 = m - 1 + (m - 1)^2\alpha - 2(1 - 2\alpha)$  and  $q_1 = \sqrt{(1 - \alpha + m\alpha)^2 - 4\alpha(1 - \alpha)}$ . Based on Lemma 2 [33] (see Appendix A), Eqs. (6) and (7), we can obtain an optimal value  $\alpha_{opt}$  of  $\alpha$  from  $\left. \frac{\partial \lambda_2^h(\alpha, m)}{\partial \alpha} \right|_{\alpha=\alpha_{opt}} = 0$ , such that  $\lambda_2^h(\alpha, m)$  reaches the maximum value at  $\alpha = \alpha_{opt} = (\sqrt{(m - 1)^3} - m + 3)/(m^2 - 2m + 5)$  since  $\partial^2 \lambda_2^h(\alpha, m)/\partial^2 \alpha < 0$ . Then, one has  $\lambda_2^h(\alpha_{opt}, m) = \left[ (m - 1)\sqrt{m^3 - 3m^2 + 3m - 1} + (2m - m^2 - 5)\sqrt{m - 1} + 2m - 2 \right] / (m^2 - 2m + 5)$ . Fig. 2(b) shows the inverted U-shaped curves of  $\lambda_2^h$  versus  $\alpha$  for various values of  $m$ , which indicates that there is an optimal solution  $\alpha_{opt}$  corresponding to the maximum value of the spectral gap  $\lambda_2^h$ .

The phase diagram in the plane  $(m, \alpha)$  for the spectral gap  $\lambda_2^h$  is illustrated in Fig. 3. In Fig. 3, the optimal coupling strength  $\alpha_{opt}$  is shown in the pentagrams, which divides the area into two parts. The top (bottom) part indicates that the lower-order (higher-order) coupling part has a greater positive impact on the spectral gap. Besides, the optimal solution  $\alpha_{opt}$  implies three aspects of the  $(m - 1)$ -order quasi-star network: (i)  $\alpha_{opt}$  is a threshold to distinguish which one of the lower-order and higher-order coupling parts has more impact on the spectral gap  $\lambda_2^h$ . Specifically, for  $\alpha < \alpha_{opt}$  ( $\alpha > \alpha_{opt}$ ),  $\lambda_2^h$  gets greater with increasing  $\alpha$  ( $a_0$ ), and then the diffusibility of the network is enhanced by increasing

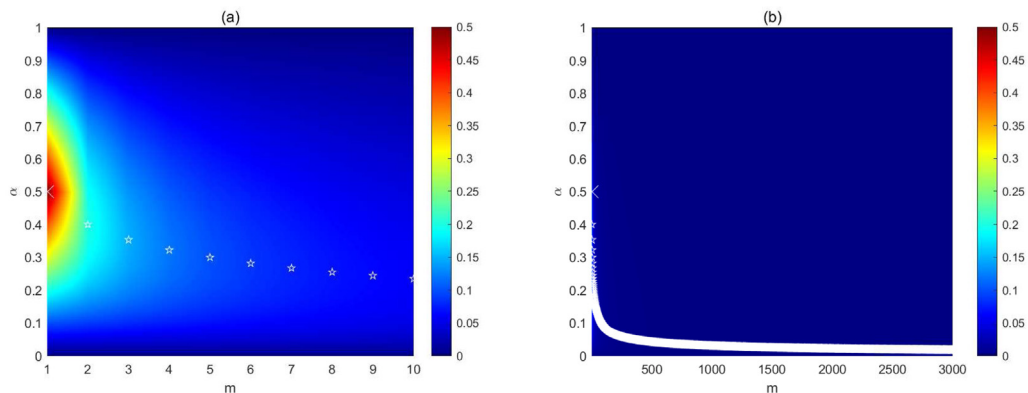


**Fig. 3.** Phase diagram for the spectral gap  $\lambda_2^h$  corresponding to an  $(m - 1)$ -order quasi-star network in the case of  $a_0 + g = 1$ . Each cross (pentagram) represents the optimal  $\alpha_{opt}$  where  $\lambda_2^h$  reaches the maximum value for  $m = 1$  ( $m > 1$ ).

the coupling strength of the higher-order (lower-order) coupling part, which is observed in Fig. 3(a). (ii)  $\alpha_{opt}$  gets smaller with increasing  $m$  since  $\frac{\partial \alpha_{opt}}{\partial m} = \frac{p_2}{q_2} < 0$ , where  $p_2 = -\frac{1}{2}\sqrt{(m - 1)^5 + 6\sqrt{m - 1} + m^2 - 6m + 1}$  and  $q_2 = (m^2 - 2m + 5)^2$ , then  $\alpha_{opt}(m) \leq \alpha_{opt}(2) = 0.4$ , and therefore the lower-order coupling part has a wider positive impact region of the spectral gap than the higher-order coupling part, as illustrated in Fig. 3(b). (iii) As shown in Fig. 3, if  $m$  is small, the size of the optimal solution  $\alpha_{opt}$  decreases rapidly with the increase of  $m$ . The rates of change of  $\alpha_{opt}$  are 0.0206 and  $7.1733 \times 10^{-4}$  if  $m$  increases from 2 to 10 and 500 respectively. When  $m$  reaches a specific level,  $\alpha_{opt}$  decreases slowly as  $m$  increases. For example, if  $m$  increases from 2 to 3000, the rate of change of  $\alpha_{opt}$  is  $1.2744 \times 10^{-4}$ . Therefore, the sensitivity of  $\alpha_{opt}$  to  $m$  decreases as  $m$  increases.

### 3.2. In the higher-order coupling part

In the higher-order coupling part,  $\lambda_2^h$  increases with the increasing of  $g$  in the regime of  $\alpha < \alpha_{opt}$ . Note that  $g$  is related to the coupling strengths  $a_1, \dots, a_{m-1}$  of the faces of the higher-order coupling part. In this subsection, we further investigate which component makes a key contribution to  $g$ .

From the definition of  $g$ , one has

$$\begin{aligned} \frac{\partial g}{\partial a_1} &= \lim_{\Delta \rightarrow 0} \frac{g(a_1 + \Delta) - g(a_1)}{\Delta} = C_{m-2}^0, \\ &\dots \\ \frac{\partial g}{\partial a_{\lceil \frac{m}{2} \rceil - 1}} &= \lim_{\Delta \rightarrow 0} \frac{g(a_{\lceil \frac{m}{2} \rceil - 1} + \Delta) - g(a_{\lceil \frac{m}{2} \rceil - 1})}{\Delta} = C_{m-2}^{\lceil \frac{m}{2} \rceil - 2}, \\ \frac{\partial g}{\partial a_{\lceil \frac{m}{2} \rceil}} &= \lim_{\Delta \rightarrow 0} \frac{g(a_{\lceil \frac{m}{2} \rceil} + \Delta) - g(a_{\lceil \frac{m}{2} \rceil})}{\Delta} = C_{m-2}^{\lceil \frac{m}{2} \rceil - 1}, \\ \frac{\partial g}{\partial a_{\lceil \frac{m}{2} \rceil + 1}} &= \lim_{\Delta \rightarrow 0} \frac{g(a_{\lceil \frac{m}{2} \rceil + 1} + \Delta) - g(a_{\lceil \frac{m}{2} \rceil + 1})}{\Delta} = C_{m-2}^{\lceil \frac{m}{2} \rceil}, \\ &\dots \\ \frac{\partial g}{\partial a_{m-1}} &= \lim_{\Delta \rightarrow 0} \frac{g(a_{m-1} + \Delta) - g(a_{m-1})}{\Delta} = C_{m-2}^{m-2}, \end{aligned} \tag{8}$$

where  $\lceil \cdot \rceil$  represents a function of rounding a number up to the next integer.

From the definition of  $g$ , we know that  $g$  is a linear combination of  $a_1, \dots, a_{m-1}$  with binomial coefficients  $C_{m-2}^0, \dots, C_{m-2}^{m-2}$ . According to the theory of composite function, the spectral gap gets greater with increasing  $a_1, \dots, a_{m-1}$ . Thus, it is concluded that: (a) For any odd number  $m$ , the spectral gap can be maximized by increasing  $a_{\lceil \frac{m}{2} \rceil - 1}$  or  $a_{\lceil \frac{m}{2} \rceil}$  because of  $C_{m-2}^{\lceil \frac{m}{2} \rceil - 2} = C_{m-2}^{\lceil \frac{m}{2} \rceil - 1} > C_{m-2}^{\lceil \frac{m}{2} \rceil - 3} = C_{m-2}^{\lceil \frac{m}{2} \rceil} > \dots > C_{m-2}^0 = C_{m-2}^{m-2}$ , as illustrated in Fig. 4(a) for  $m = 9$ . The red dotted line indicates a threshold value  $a_{thr} = 0.0067$ , that is, when  $a_4 \in (0, 0.01]$  or  $a_5 \in (0, 0.01]$ , the spectral gap value  $\lambda_2^h(a_4) = \lambda_2^h(a_5) = 0.0639$  corresponding to  $a_4 = 0.0067$  or  $a_5 = 0.0067$  is the largest. In addition, their spectral gap values are larger than those corresponding to  $a_1, a_2, a_3, a_6, a_7$  and  $a_8$ . (b) Similarly, for any even number  $m$ ,  $\frac{m}{2}$ -order

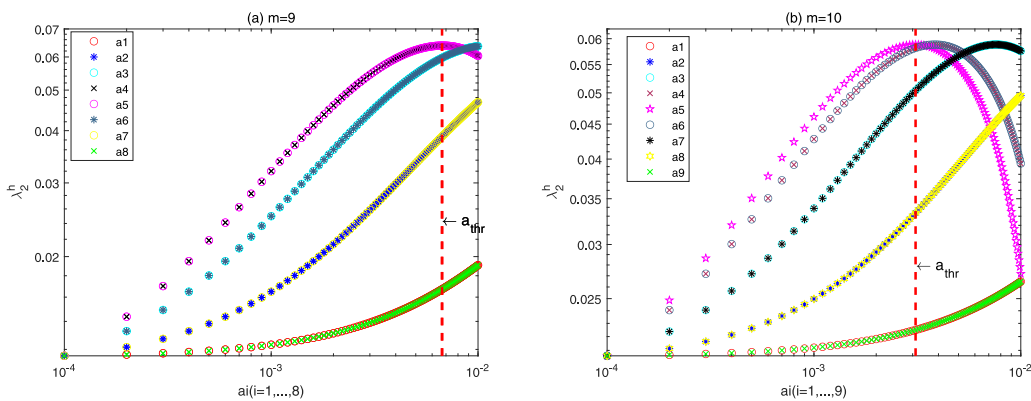


**Fig. 4.** Relation between  $\lambda_2^h$  and  $a_i$  under  $a_0 = 1 - \sum_{k=1}^{m-1} a_k C_{m-2}^{k-1}$  for  $m = 9$  (a) and  $m = 10$  (b), respectively. The red dotted lines indicate the threshold value  $a_{thr}$  of  $a_i$  such that  $\lambda_2^h$  reaches the maximum value at  $a_i = a_{thr}$ .

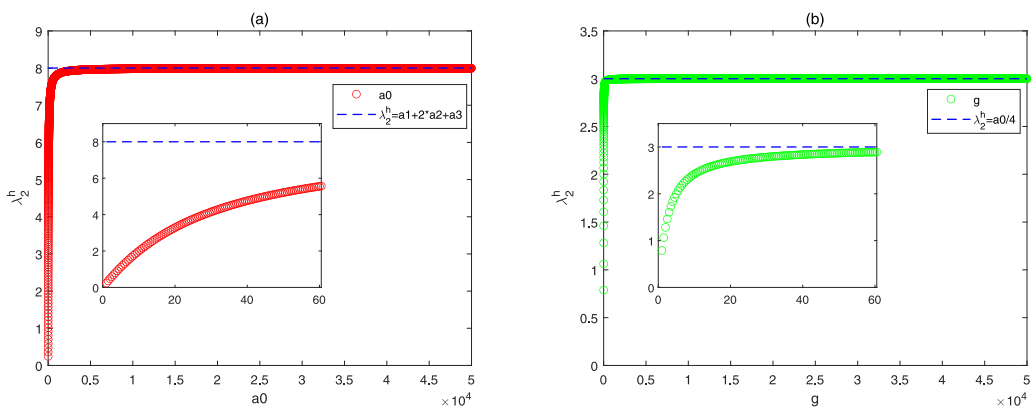


**Fig. 5.** The spectral gap  $\lambda_2^h$  as a function of  $a_0$  with  $g = 8$  (a) and  $g$  with  $a_0 = 12$  (b) respectively.

face is the most conducive to enhance the diffusibility of the network, as shown in Fig. 4(b) for  $m = 10$ . At this time, the maximum spectral gap value corresponding to the threshold  $a_{thr} = 0.0031$  is  $\lambda_2^h(a_5) = 0.0588$ . The results show that more nodes in a single face do not necessarily improve the diffusibility of a higher-order network.

#### 4. Case II: $a_0 \gg 1$ and $g \gg 1$

In this section, the case of  $a_0 \gg 1$  and  $g \gg 1$  is considered.

##### 4.1. The lower-order and higher-order coupling parts

According to Eq. (4), one has

$$\frac{\partial \lambda_2^h}{\partial a_0} = \frac{1}{2} - \frac{p_3}{2\sqrt{\Delta_1}}, \tag{9}$$

where  $p_3 = a_0 + mg - 2g$ . Then  $\partial \lambda_2^h / \partial a_0 > 0$  since  $|\sqrt{\Delta_1}| \geq |p_3|$  holds for any  $g > 0$  and  $m \geq 2$ . Moreover,  $\lim_{a_0 \rightarrow +\infty} \lambda_2^h = g = \sum_{k=1}^{m-1} a_k C_{m-2}^{k-1}$ . Therefore, the spectral gap  $\lambda_2^h$  is a monotonically increasing function of  $a_0$ , and tends to the upper bound  $g$  as  $a_0$  approaches the infinity. Fig. 5(a) displays the relation between  $\lambda_2^h$  and  $a_0$  for the 3-order quasi-star network shown in Fig. 1. From Fig. 5(a), we observe that  $\lambda_2^h$  converges to an upper bound  $a_1 + 2a_2 + a_3$ , which is consistent with the above analytic result.

On the other hand, from Eq. (4), we also get

$$\frac{\partial \lambda_2^h}{\partial g} = \frac{m}{2} - \frac{q_3}{2\sqrt{\Delta_1}}, \tag{10}$$

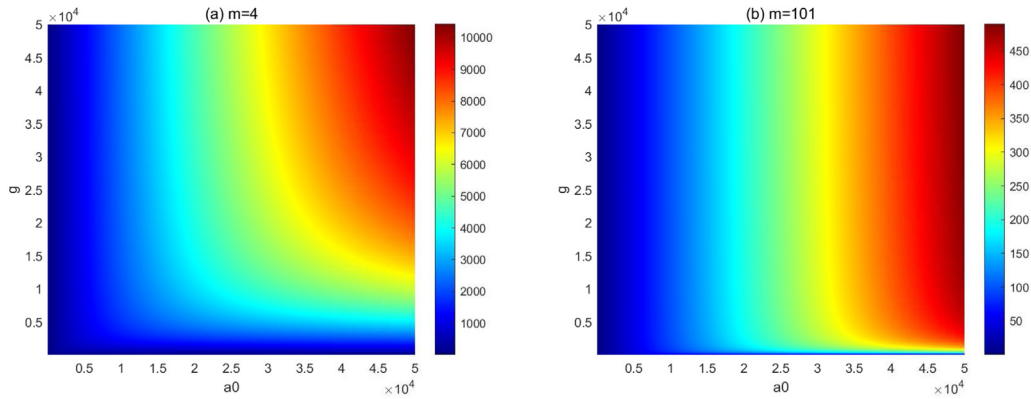


Fig. 6. The spectral gap  $\lambda_2^h$  as a function of  $a_0$  and  $g$  for  $m = 4$  (a) and  $m = 101$  (b) respectively.

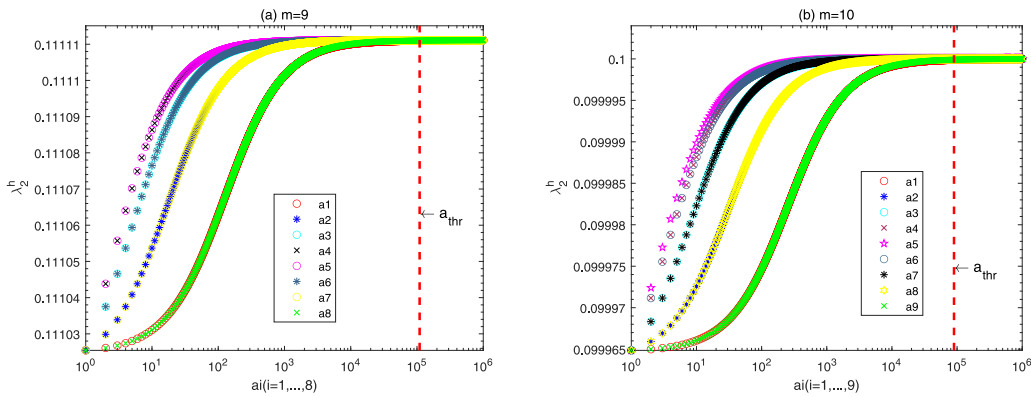


Fig. 7. The spectral gap  $\lambda_2^h$  versus  $a_i$  for  $m = 9$  (a) and  $m = 10$  (b) respectively, where  $a_j = 1, a_0 = 1, j \neq i$ .

where  $q_3 = m(a_0 + mg) - 2a_0$ . Due to  $|m\sqrt{\Delta_1}| \geq |q_3|$  for any  $g > 0$  and  $m \geq 2$ , then  $\partial\lambda_2^h/\partial g > 0$ . It is further deduced that  $\lim_{g \rightarrow +\infty} \lambda_2^h = a_0/m$ . As a result,  $\lambda_2^h$  is monotonically increasing with respect to  $g$ , and has an upper bound  $a_0/m$ , as is seen in Fig. 5(b).

Fig. 6 depicts the spectral gap  $\lambda_2^h$  of the  $(m - 1)$ -order quasi-star network in terms of  $a_0$  and  $g$  for  $m = 4$  and  $m = 101$ . It is seen from Fig. 6 that the larger  $a_0$  or  $g$ , the larger  $\lambda_2^h$ , in turn, the stronger the diffusibility of the network. Besides, we conclude that the variation of  $a_0$  brings about a greater change of  $\lambda_2^h$  than that of  $g$ .

#### 4.2. In the higher-order coupling part

When  $g \gg 1$ ,  $\lambda_2^h$  gets greater with increasing  $g$ . Since  $g$  is dependent on  $a_i$  ( $i = 1, \dots, m - 1$ ), we explore the impact of  $a_i$  on  $\lambda_2^h$  in the higher-order coupling part. It is obtained that  $\lim_{a_i \rightarrow +\infty} \lambda_2^h = a_0/m$  and  $\frac{\partial g}{\partial a_1} > 0, \frac{\partial g}{\partial a_2} > 0, \dots, \frac{\partial g}{\partial a_{m-1}} > 0$ . Thus  $\lambda_2^h$  gets greater with increasing the coupling strength  $a_i$  of a face of the higher-order coupling part. For any odd number  $m$ , the  $(\lceil \frac{m}{2} \rceil - 1)$ -order or  $\lceil \frac{m}{2} \rceil$ -order face, rather than any other face, has more impact on the spectral gap since  $C_{m-2}^{\lceil \frac{m}{2} \rceil - 2} = C_{m-2}^{\lceil \frac{m}{2} \rceil - 1} > C_{m-2}^{\lceil \frac{m}{2} \rceil - 3} = C_{m-2}^{\lceil \frac{m}{2} \rceil} > \dots > C_{m-2}^0 = C_{m-2}^{m-2}$ . Additionally,  $\lambda_2^h$  increases with  $a_i$  ( $i = 1, 2, \dots, m - 1$ ), and has almost the same upper bounded value  $a_0/m$  when  $a_i > a_{thr}$ , as shown in Fig. 7(a). Similarly, for any even number  $m$ , the  $\frac{m}{2}$ -order face has more impact on the spectral gap, and if every  $a_i$  ( $i = 1, 2, \dots, m - 1$ ) is greater than the threshold  $a_{thr}$ , then their corresponding diffusibility are almost equal, as shown in Fig. 7(b). The red dotted lines in Fig. 7(a) and (b) respectively represent the threshold  $a_{thr}$  for  $m = 9$  and  $m = 10$ . On the left side of these red dotted lines, the spectral gap increases slowly with the increase of the coupling strength of a single face. While on the other side of the red dotted lines, these corresponding spectral gap values are almost the same, which is consistent with our results.

### 5. Further discussion

We further extend the higher-order coupling parts to simplexes with various orders based on the aforementioned results, and discover some interesting phenomena. For an  $(m - 1)$ -order quasi-star network with  $T$  simplexes shown

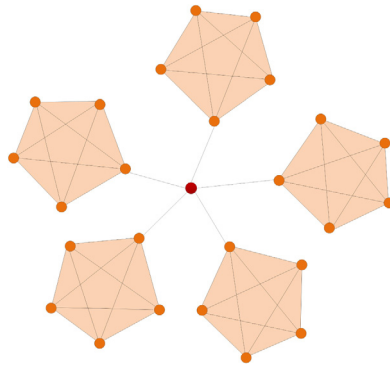


**Fig. 8.** A quasi-star network with 5 4-order simplexes, where  $\lambda_2^h = 0.1849$  with multiplicity 4,  $T = 5$  and  $m - 1 = 4$ .

in Fig. 8 ( $T = 5$ ,  $m - 1 = 4$ ),  $\lambda_2^h$  is the second smallest Laplacian eigenvalue with multiplicity  $T - 1$ . If  $T_2$  ( $T_2 < T$ )  $(m - 1)$ -order simplexes are replaced by  $T_2$   $k$ -order ( $k < m - 1$ ) simplexes, the second smallest Laplacian eigenvalue is the same as that of the original network, but its multiplicity is reduced by  $T_2$ . For example,  $\lambda_2^h$  is  $\lambda_2^h = 0.1849$  with multiplicity 4 in Fig. 8. The detailed changes of the network topologies and the spectral gaps are illustrated in Figure B1 and Table 1 (see Appendix B). As shown in Table 1, if a 4-order simplex is replaced with a 3-order simplex or a 2-order simplex in Figure B1-1(a), B1-1(b),  $\lambda_2^h$  is still the second smallest Laplacian eigenvalue, but its multiplicity is 3, where  $T_1 = 4$ ,  $T_2 = 1$ . Similarly, if two (three) 4-order simplexes are all replaced by two (three) 3-order simplexes or 2-order simplexes in Figure B1-2(a), B1-2(b) (Figure B1-3(a), B1-3(b)),  $\lambda_2^h$  is still the second smallest Laplacian eigenvalue, but its multiplicity is 2 (1), where  $T_1 = 3$ ,  $T_2 = 2$  ( $T_1 = 2$ ,  $T_2 = 3$ ). As a result, the diffusibility of a quasi-star network may be unchanged if part of the order numbers of the higher-order coupling decrease.

## 6. Conclusion

This paper studies the diffusibility of a kind of quasi-star higher-order network and discusses the impact of the lower-order and higher-order coupling parts on the diffusibility. When the coupling strengths of the lower-order and higher-order coupling parts are less than 1, the diffusibility of the quasi-star networks can reach the maximum value at some intermediate values of  $a_0$  and  $g$ . In addition, if  $g$  is smaller than a certain threshold, compared with other components of  $g$ , increasing  $a_{\lceil \frac{m}{2} \rceil}$  in the higher-order coupling part has a greater advantage in enhancing the diffusibility of the quasi-star networks, and their diffusibility does not always improve with the order of a face. On the other hand, when  $a_0 \gg 1$  and  $g \gg 1$ , there exist upper bounds of the spectral gaps, that is  $g$  and  $a_0/m$ , and the effect of the lower-order coupling part on the network's diffusibility is greater than that of the higher-order coupling part. Similarly, the  $\lceil \frac{m}{2} \rceil$ -order face also has an important impact on the network's diffusibility in the higher-order coupling part than any other face. Further work includes more general quasi-star higher-order network, where the higher-order coupling parts consist of various orders simplexes, and the impact of higher-order interactions on multilayer higher-order networks.

## CRedit authorship contribution statement

**Bo Li:** Conceptualization, Methodology, Software, Formal analysis, Investigation, Writing – original draft, Funding acquisition. **Jin Zhou:** Methodology, Formal analysis, Writing – original draft, Funding acquisition. **Weiqiang Li:** Software, Formal analysis, Data curation, Writing – original draft. **Jun-an Lu:** Methodology, Software, Data curation, Writing – original draft.

## Declaration of competing interest

The authors declare that they have no known competing financial interests or personal relationships that could have appeared to influence the work reported in this paper.

## Data availability

No data was used for the research described in the article.

## Acknowledgments

This work is supported by the National Natural Science Foundation of China under Grant 62173254 and the National Key Research and Development Program of China (No. 2020YFA0714200).

**Appendix A**

**Lemma 1** ([32]). Let  $A$  be an  $m$  by  $m$  square matrix,  $B$  an  $m$  by  $n$  matrix,  $C$  an  $n$  by  $n$  square matrix, and  $\mathbf{0}$  an  $n$  by  $m$  matrix with each element being 0. Then

$$\begin{vmatrix} A_{m \times m} & B_{m \times n} \\ \mathbf{0}_{n \times m} & C_{n \times n} \end{vmatrix} = |A| |C|.$$

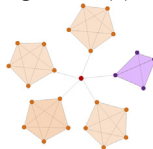
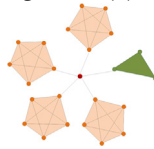
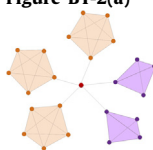
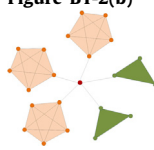
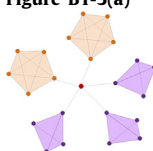
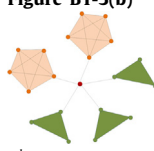
**Lemma 2** ([33]). Suppose that  $f'(x_0) = 0$ .

- (1) If  $f''(x_0) < 0$ , then  $f(x_0)$  is a maximum value.
- (2) If  $f''(x_0) > 0$ , then  $f(x_0)$  is a minimum value.

**Appendix B**

See Table 1.

**Table 1**  
Eigenvalues of the multi-order Laplacian matrix  $\mathcal{L}$  with  $T = T_1 + T_2 = 5$ .

$T_1 = 4,$ $T_2 = 1$	$\lambda_2^h$ with multiplicity 3	<p><b>Figure B1-1(a)</b></p>  <p><math>\lambda_{2,3,4}^h = 0.1849,</math> <math>\lambda_5^h = 0.2194, \dots</math></p>	<p><b>Figure B1-1(b)</b></p>  <p><math>\lambda_{2,3,4}^h = 0.1849,</math> <math>\lambda_5^h = 0.2759, \dots</math></p>
$T_1 = 3,$ $T_2 = 2$	$\lambda_2^h$ with multiplicity 2	<p><b>Figure B1-2(a)</b></p>  <p><math>\lambda_{2,3}^h = 0.1849,</math> <math>\lambda_4^h = 0.2108, \dots</math></p>	<p><b>Figure B1-2(b)</b></p>  <p><math>\lambda_{2,3}^h = 0.1849,</math> <math>\lambda_4^h = 0.2533, \dots</math></p>
$T_1 = 2,$ $T_2 = 3$	$\lambda_2^h$ with multiplicity 1	<p><b>Figure B1-3(a)</b></p>  <p><math>\lambda_2^h = 0.1849,</math> <math>\lambda_3^h = 0.2022, \dots</math></p>	<p><b>Figure B1-3(b)</b></p>  <p><math>\lambda_2^h = 0.1849,</math> <math>\lambda_3^h = 0.2306, \dots</math></p>

**References**

- [1] Shen Y, Liu X. Generalized synchronization of delayed complex-valued dynamical networks via hybrid control. *Commun Nonlinear Sci Numer Simul* 2023;118:107057.
- [2] Zhou J, Chen J, Lu J, Lü J. On applicability of auxiliary system approach to detect generalized synchronization in complex network. *IEEE Trans Automat Control* 2017;62(7):3468–73.
- [3] Zhu S, Zhou J, Lü J, Lu J. Finite-time synchronization of impulsive dynamical networks with strong nonlinearity. *IEEE Trans Automat Control* 2021;66(8):3550–61.
- [4] Xu M, Zhou J, Lu J, Wu X. Synchronizability of two-layer networks. *Eur Phys J B* 2015;88(9):240.
- [5] Ma J, Li F, Huang L, Jin W. Complete synchronization, phase synchronization and parameters estimation in a realistic chaotic system. *Commun Nonlinear Sci Numer Simul* 2011;16(9):3770–85.
- [6] Manshaei MH, Zhu Q, Alpcan T, Basar T, Hubaux JP. Game theory meets network security and privacy. *ACM Comput Surv* 2013;45(3):25.
- [7] Tejedor A, Longjas A, Fofoula-georgiou E, Georgiou TT, Moreno Y. Diffusion dynamics and optimal coupling in multiplex networks with directed layers. *Phys Rev X* 2018;8(3):031071.
- [8] Chen C, Zhou J, Qu F, Song C, Zhu S. Identifying partial topology of complex networks with stochastic perturbations and time delay. *Commun Nonlinear Sci Numer Simul* 2023;115:106779.
- [9] Li W, Zhou J, Jin Z, Lu J. The combination of targeted vaccination and ring vaccination. *Chaos* 2021;31(6):063108.

- [10] Borromean Rings. <https://mathcurve.com/courbes3d.gb/borromee/borromee.shtml>.
- [11] Bianconi G. Higher-order networks. Elements in structure and dynamics of complex networks. Cambridge University Press; 2021.
- [12] Bretto A. Hypergraph theory. An introduction. Mathematical engineering. Cham: Springer; 2013.
- [13] Shi D, Chen G. Simplicial networks: a powerful tool for characterizing higher-order interactions. *Natl Sci Rev* 2022;9(5):nwac038.
- [14] Shi D, Chen Z, Sun X, Chen Q, Ma C, Lou Y, et al. Computing cliques and cavities in networks. *Commun Phys* 2021;4(1):249.
- [15] Fan T, Lü L, Shi D, Zhou T. Characterizing cycle structure in complex networks. *Commun Phys* 2021;4(1):272.
- [16] Battiston F, Cencetti G, Iacopini I, Latora V, Lucas M, Patania A, et al. Networks beyond pairwise interactions: structure and dynamics. *Phys Rep* 2020;874:1–92.
- [17] Chen G. Searching for best network topologies with optimal synchronizability: a brief review. *IEEE/CAA J Autom Sin* 2022;9(4):573–7.
- [18] Gambuzza LV, Di-patti F, Gallo L, Lepri S, Romance M, Criado R, et al. Stability of synchronization in simplicial complexes. *Nature Commun* 2021;12(1):1255.
- [19] Gallo L, Muolo R, Gambuzza LV, Latora V, Frasca M, Carletti T. Synchronization induced by directed higher-order interactions. *Commun Phys* 2022;5(1):263.
- [20] Lucas M, Cencetti G, Battiston F. Multiorder laplacian for synchronization in higher-order networks. *Phys Rev Res* 2020;2(3):033410.
- [21] Torres JJ, Bianconi G. Simplicial complexes: higher-order spectral dimension and dynamics. *J Phys-Complexity* 2020;1(1):015002.
- [22] Fiedler M. Algebraic connectivity of graphs. *Czech Math J* 1973;23(2):298–305.
- [23] Shang Y. A system model of three-body interactions in complex networks: consensus and conservation. *P Roy Soc A-Math Phy* 2022;478(2258):20210564.
- [24] Arenas A, Diaz-guilera A, Perez-vicente CJ. Synchronization processes in complex networks. *Physica D* 2006;224(1–2):27–34.
- [25] Gomez S, Diaz-guilera A, Gomez-gardenes J, Perez-vicente CJ, Moreno Y, Arenas A. Diffusion dynamics on multiplex networks. *Phys Rev Lett* 2013;110(2):028701.
- [26] Sizemore AE, Giusti C, Kahn A, Vettel JM, Betzel RF, Bassett DS. Cliques and cavities in the human connectome. *J Comput Neurosci* 2018;44(1):115–45.
- [27] Kang L, Wang Z, Huo S, Tian C, Liu Z. Remote synchronization in human cerebral cortex network with identical oscillators. *Nonlinear Dynam* 2020;99(2):1577–86.
- [28] Bergner A, Frasca M, Sciuto G, Buscarino A, Ngamga EJ, Fortuna L, et al. Remote synchronization in star networks. *Phys Rev E* 2012;85(2):026208.
- [29] Zhang Y, Latora V, Motter AE. Unified treatment of synchronization patterns in generalized networks with higher-order, multilayer, and temporal interactions. *Commun Phys* 2021;4(1):195.
- [30] Courtney OT, Bianconi G. Generalized network structures: the configuration model and the canonical ensemble of simplicial complexes. *Phys Rev E* 2016;93(6):062311.
- [31] Shang Y. Non-linear consensus dynamics on temporal hypergraphs with random noisy higher-order interactions. *J Complex Netw* 2023;11(2):cnad009.
- [32] Zhang F. Matrix theory: Basic results and techniques. New York: Springer; 2011, p. 37–8.
- [33] Ouyang G, Zhu X, Jin F, Chen C. Mathematical analysis. 3rd ed. Higher Education Press; 2006.